Title

Neural network dynamics underlying gamma synchronization deficits in schizophrenia

Authors

Koshiyama, Daisuke
Miyakoshi, Makoto
Joshi, Yash B
et al.

Publication Date

2021-04-01

DOI

10.1016/j.pnpbp.2020.110224

Peer reviewed

Published in final edited form as:

Prog Neuropsychopharmacol Biol Psychiatry. 2021 April 20; 107: 110224. doi:10.1016/j.pnpbp.2020.110224.

Neural network dynamics underlying gamma synchronization deficits in schizophrenia

Daisuke Koshiyama[a], **Makoto Miyakoshi**[b,*], **Yash B. Joshi**[a,c], **Juan L. Molina**[a,c], **Kumiko Tanaka-Koshiyama**[a], **Joyce Sprock**[a,c], **David L. Braff**[a,c], **Neal R. Swerdlow**[a], **Gregory A. Light**[a,c]

[a]Department of Psychiatry, University of California San Diego, La Jolla, CA 92093-0804, USA

[b]Swartz Center for Neural Computation, University of California San Diego, La Jolla, CA 92093-0559, USA

[c]VISN-22 Mental Illness, Research, Education and Clinical Center (MIRECC), VA San Diego Healthcare System, San Diego, CA 92161, USA

Abstract

Gamma-band (40-Hz) activity is critical for cortico-cortical transmission and the integration of information across neural networks during sensory and cognitive processing. Patients with schizophrenia show selective reductions in the capacity to support synchronized gamma-band oscillations in response to auditory stimulation presented 40-Hz. Despite widespread application of this 40-Hz auditory steady-state response (ASSR) as a translational electroencephalographic biomarker for therapeutic development for neuropsychiatric disorders, the spatiotemporal dynamics underlying the ASSR have not been fully characterized. In this study, a novel Granger causality analysis was applied to assess the propagation of gamma oscillations in response to 40-Hz steady-state stimulation across cortical sources in schizophrenia patients ($n = 426$) and healthy comparison subjects ($n = 293$). Both groups showed multiple ASSR source interactions that were broadly distributed across brain regions. Schizophrenia patients showed distinct, hierarchically sequenced connectivity abnormalities. During the response onset interval, patients exhibited abnormal increased connectivity from the inferior frontal gyrus to the superior temporal gyrus, followed by decreased connectivity from the superior temporal to the middle cingulate gyrus. In the later portion of the ASSR response (300–500 ms), patients showed significantly increased connectivity from the superior temporal to the middle frontal gyrus followed by decreased connectivity from the left superior frontal gyrus to the right superior and middle frontal gyri. These findings highlight both the orchestration of distributed multiple sources in response to simple gamma-frequency stimulation in healthy subjects as well as the patterns of deficits in the

*Corresponding author at: Swartz Center for Neural Computation, University of California San Diego, Mail Code: 0559 9500 Gilman Drive, La Jolla, CA 92093-0559, USA. mmiyakoshi@ucsd.edu (M. Miyakoshi).

Declaration of Competing Interest

G.A. Light reported consulting for Astellas Pharma, Inc, Heptares Therapeutics, NeuroSig, Neurocrine, and Novartis.

Ethical statement

Written informed consent was obtained from each subject. The Institutional Review Board of University of California San Diego approved all experimental procedures (071128, 071831, 170147). The current study was conducted in accordance with the Declaration of Helsinki.

Supplementary data to this article can be found online at https://doi.org/10.1016/j.pnpbp.2020.110224.

generation and maintenance of gamma-band oscillations across the temporo-frontal sources in schizophrenia patients.

Keywords

Gamma-band auditory steady-state response; Effective connectivity; Source-level analysis; Schizophrenia; Neural temporal dynamics

1. Introduction

Neurophysiologic measures of early sensory information processing have a long history in characterizing fundamental schizophrenia deficits with direct and indirect functional significance (Braff et al., 1978; Braff, 1993; Kwon et al., 1999; Light and Braff, 2005). Recent advances in neuroscience have illuminated the time-linked mechanisms by which anatomically distinct brain regions communicate in order to integrate and coordinate perception, information processing, and cognition in mammals. In particular, synchronous neural oscillations in the 30–50 Hz gamma frequency range are a fundamental central nervous system (CNS) resonance frequency that is critical for communication across multiple brain regions, supporting cognitive information processing (Galuske et al., 2019; Hagoort et al., 2004; Joliot et al., 1994; Miltner et al., 1999; Rodriguez et al., 1999; Spellman et al., 2015; Traub et al., 1996). Abnormalities in synchronous neural oscillations help to explain cognitive deficits in complex brain illnesses like schizophrenia (Gandal et al., 2012; Sun et al., 2011; Uhlhaas and Singer, 2015). Since gamma synchrony measured by electroencephalography (EEG) is related with sensory, clinical, cognitive, and psychosocial functioning in schizophrenia patients (Hirano et al., 2015; Spencer et al., 2004; Uhlhaas et al., 2008; Uhlhaas and Singer, 2010), a fundamental problem in the ability to support “timing or sequencing component of mental activity” may underlie the heterogeneous constellation of clinical and cognitive deficits observed in schizophrenia patients (Andreasen, 1999).

The capacity to support the synchronous generation of neural activity can be more directly interrogated by using paradigms that aim to “entrain” oscillations at particular frequencies. For example, when receiving periodic stimulation, neural networks behave like tuned oscillators with EEG synchronizing to the frequency of stimulation (Galambos and Makeig, 1992; Galambos et al., 1981; Makeig, 1993). Schizophrenia patients have selectively reduced synchrony to auditory-based 40-Hz stimulation, but normal responses to other rates of stimulation (Brenner et al., 2003; Edgar et al., 2014; Hamm et al., 2015; Hirano et al., 2015; Koshiyama et al., 2018b, 2018c, 2019; Kwon et al., 1999; Light et al., 2006; Spencer et al., 2008; Tada et al., 2016; Teale et al., 2008; Thune et al., 2016; Tsuchimoto et al., 2011; Vierling-Claassen et al., 2008; Wilson et al., 2008). This gamma-band auditory-steady response (ASSR) has received significant attention as a potential translational biomarker in the development of novel pro-cognitive interventions for schizophrenia and other brain disorders, such as bipolar disorder, autism spectrum disorder, and 22q11.2 deletion syndrome (Desai et al., 2020; Edgar et al., 2016; Isomura et al., 2016;

Larsen et al., 2018; Light et al., 2017; Molina et al., 2020; O'Donnell et al., 2004; Oda et al., 2012; Rass et al., 2010; Reite et al., 2009; Spencer et al., 2008; Wilson et al., 2008).

Gamma oscillations are evoked by synaptic interactions between parvalbumin-positive γ-aminobutyric acid (GABA)-ergic interneurons and pyramidal neurons (Cardin et al., 2009; Sohal et al., 2009). Post-mortem brain studies in schizophrenia patients have demonstrated abnormalities in parvalbumin-positive GABAergic interneurons, such as reduced expression of the GABA-synthesizing enzyme glutamic acid decarboxylase 67 (GAD67; Akbarian and Huang, 2006) and parvalbumin (Eyles et al., 2002) in cortical interneurons. Furthermore, altered *N*-methyl-D-aspartate (NMDA) receptor signaling onto parvalbumin-positive interneurons results in gamma oscillation deficits in cortical microcircuits in animal models of schizophrenia (Carlen et al., 2012; Nakao and Nakazawa, 2014). Thus, GABAergic interneuron dysfunction in schizophrenia has a tight relationship with impaired gamma oscillations evoked in response to steady-state stimulation (Fisahn et al., 2009; Gonzalez-Burgos et al., 2015). Translating previous findings in clinical studies to animal model studies improves the potential use of ASSR translational biomarkers in the development of novel therapeutics for CNS disorders (Kozono et al., 2019).

While cellular studies of gamma oscillations indicate prominent roles of GABAergic and glutamatergic neurons, the macro organization/coordination of how these microcircuits interact across brain regions to produce the ASSR has not been comprehensively characterized. Recently, we identified the right superior temporal and orbitofrontal gyri as primary contributing sources of ASSR in both healthy subjects and schizophrenia patients. Schizophrenia patients, however, showed significant reductions in the dipole density of gamma-band ASSR in the left superior temporal gyrus, orbitofrontal cortex, and left superior frontal gyrus (Koshiyama et al., 2020e). Although this dipole mapping demonstrates the presence of a distributed network, the spatial and temporal interactions among these brain regions are unknown.

Reports suggest the ASSR response period may reflect distinct aspects of information processing and impairments in schizophrenia. Specifically, the 40-Hz ASSR is usually measured across a full 500 ms stimulation interval, with an early ~1–200 ms stimulus onset interval, and late ~300–500 ms maintenance interval (Koshiyama et al., 2018b; Tada et al., 2016): both first-episode as well as chronic schizophrenia patients have gamma-band ASSR deficits across the early and later time intervals, but individuals at clinical high-risk for psychosis showed deficits in only the later maintenance time interval (Koshiyama et al., 2018b; Light et al., 2006; Tada et al., 2016). Similarly, differential sensitivity to acute pharmacologic challenges across the time course of ASSR has been observed in both healthy subjects and patients with schizophrenia (Light et al., 2017). According to previous magnetic resonance imaging (MRI) studies, patients with first-episode schizophrenia show more severe volume reductions in the superior temporal gyrus than individuals at clinical high-risk (Chan et al., 2011). Additionally, patients with first-episode schizophrenia show progressive volume reductions in the superior temporal gyrus (Kasai et al., 2003a, 2003b). Furthermore, chronic schizophrenia patients demonstrate more severe volume reductions in the frontal cortex compared to first-episode schizophrenia. Given these previous findings and gamma-band ASSR reflects early auditory information processing, gamma-band ASSR

may propagate from the superior temporal gyrus including primary auditory cortex to the frontal regions.

Augmenting MRI-based studies of *structural* connectivity, gamma-band ASSR can leverage the functional fine temporal resolution of EEG to assess *effective* connectivity, i.e., the causal interactions (i.e., directed connectivities) among underlying brain regions that generate and maintain 40-Hz ASSR. This study, therefore, aimed to extend our previous dipole density analysis via the application of a novel, data-driven Granger causality (Granger, 1969) analysis to deconstruct the time course and patterns of effective connectivity of cortical sources underlying the 40-Hz ASSR and its deficits in the same archival sample of healthy subjects and schizophrenia patients (Koshiyama et al., 2020e). This Granger causality approach identifies causal interactions among brain regions that generate and maintain 40-Hz ASSR represented as effective connectivity between two nodes using a correlation with time delay of EEG phase activity at the pair of nodes. Using this novel approach, we aimed to show temporal and spatial dynamics of information processing underlying 40-Hz ASSR. In addition to the early and later time intervals, we also characterized the middle time interval of the response, representing the transitional period between the response generation and maintenance phases.

2. Methods

2.1. Subjects

Participants were 426 schizophrenia patients and 293 healthy comparison subjects (Table 1). Source-level and conventional scalp-level ASSR measures in this cohort were previously reported (Koshiyama et al., 2020b, 2020d, 2020e, 2020f). Patients were recruited from community residential facilities and via clinician referral, and diagnosed using a modified version of the Structured Clinical Interview for DSM-IV-TR. Antipsychotic medications were prescribed for 388 schizophrenia patients. Healthy comparison subjects were recruited through internet advertisements. Exclusion criteria included an inability to understand the consent processes and/or provide consent or assent, not being a fluent English speaker, previous significant head injury with loss of consciousness, neurologic illness, or severe systemic illness. Written informed consent was obtained from each subject. Audiometric testing was used to ensure that all participants could detect 1000-Hz tones at 40 dB. The Institutional Review Board of University of California San Diego approved all experimental procedures (071128, 071831, 170147). The current study was conducted in accordance with the Declaration of Helsinki.

2.2. Stimuli and procedures

Auditory steady-state stimuli were presented to subjects by means of foam insert earphones (Model 3A; Aearo Company Auditory Systems, Indianapolis, Indiana). The stimuli were 1-millisecond, 93-dB clicks presented at 40 Hz in 500-millisecond trains. A block typically contained 200 trains of the clicks with 500-millisecond intervals. During the session, participants watched a silent cartoon video.

2.3. Electroencephalography recording and preprocessing

EEG data were continuously digitized at a rate of 1000 Hz (nose reference, forehead ground) using a 40-channel Neuroscan system (Neuroscan Laboratories, El Paso, Texas). The electrode montage was based on standard positions in the International 10–5 electrode system (Oostenveld and Praamstra, 2001) to fit the Montreal Neurological Institute (MNI) template head used in EEGLAB, including AFp10 and AFp9 as horizontal electro-oculographic (EOG) channels, IEOG and SEOG above and below the left eye as vertical EOG channels, Fp1, Fp2, F7, F8, Fz, F3, F4, FC1, FC2, FC5, FC6, C3, Cz, C4, CP1, CP2, CP5, CP6, P7, P3, Pz, P4, P8, T7, T8, TP9, TP10, FT9, FT10, PO9, PO10, O1, O2, and Iz. Electrode-to-skin impedance mediated by conductive gel was brought below 4 kΩ. The system acquisition band pass was 0.5–100 Hz. Offline, EEG data were imported to EEGLAB 14.1.2 (Delorme and Makeig, 2004) running under Matlab 2017b (The MathWorks, Natick, MA). Data were high-pass filtered (finite impulse response (FIR), Hamming window, cutoff frequency 0.5 Hz, transition bandwidth 0.5). EEGLAB plugin *clean_rawdata()* including Artifact Subspace Reconstruction (ASR) was applied to reduce high-amplitude artifacts (Blum et al., 2019; Chang et al., 2018, 2020; Gabard-Durnam et al., 2018; Kothe and Makeig, 2013; Mullen et al., 2015). The parameters used were: flat line removal, 10 s; electrode correlation, 0.7; ASR, 20; window rejection, 0.5. Mean channel rejection rate was 4.2% (SD 2.3, range 0–15.8). Mean data rejection rate was 2.0% (SD 3.5, range 0–22.4). The rejected channels were interpolated using EEGLAB's spline interpolation function. Data were re-referenced to average. Adaptive mixture independent component analysis (ICA; Delorme et al., 2012) was applied to the preprocessed scalp recording data to obtain temporally maximally independent components (ICs). For scalp topography of each IC derived, equivalent current dipole was estimated using Fieldtrip functions (Oostenveld et al., 2011). For scalp topographies more suitable for symmetrical bilateral dipoles, two symmetrical dipoles were estimated (Piazza et al., 2016). To select brain ICs among all types of ICs, EEGLAB plugin *ICLabel()* was used (Pion-Tonachini et al., 2019). The inclusion criteria were 1) 'brain' label probability >0.7 and 2) residual variance i.e., var.((actual scalp topography) – (theoretical scalp projection from the fitted dipole))/var.(actual scalp topography) < 0.15. Continuous EEG data were segmented into epochs that started at −250 ms and end at 750 ms relative to stimulus onset. Epoch rejection was performed for each participant using their median value of single-trial power spectral density (PSD) of remaining ICs. The single-trial PSD values were calculated and the median value across trials was subtracted. The residual errors from the median were z-scored. Any epoch with mean value >2 between 15 and 35 Hz was rejected as contaminated by muscle potentials. The final processed data had a mean of 158.6 trials (SD 18.4).

2.4. Effective connectivity analyses

To calculate the grand-mean effective connectivity across ICs for each group, we applied EEGLAB plugin groupSIFT, which recently demonstrated successful application in other clinical EEG projects (Koshiyama et al., 2020a, 2020d; Loo et al., 2019). Using n = 9324 ICs that were classified as brain ICs (mean 13.0 ICs per person, SD 4.4, range 4–28), time-frequency decomposed renormalized partial directed coherence (RPDC; Schelter et al., 2009) was calculated across ICs (sliding window length 0.3 s, window step size 4 ms, logarithmically distributing 50 frequency bins from 2 to 55 Hz, baseline period

−0.1 to 0 s). This generated a connectivity matrix with the dimension of IC × IC for each individual. The grand-average optimum model order was 11.6 (SD 1.6), i.e. delayed effective connectivity up to about 48 ms was utilized. The estimated equivalent dipole locations of the corresponding ICs were convolved with 3-D Gaussian kernel with 20 mm full width at half maximum (FWHM) to obtain a probabilistic dipole density. The dipole density inside the brain space is segmented into anatomical regions defined by automated anatomical labeling (AAL; Tzourio-Mazoyer et al., 2002). The original AAL has 88 anatomical regions, but those basal and limbic regions that are unlikely to be scalp-measured EEG sources were integrated into two umbrella terms, upper basal and lower basal. The vagueness was intentional to avoid a potential misrepresentation of limbic/basal EEG sources.

Notably, the original labels of groupSIFT ‘upper basal’ and ‘lower basal’ were reported as the ventral mid-cingulate gyrus, ‘mid-cingulate’ as the dorsal mid-cingulate gyrus, ‘insula’ as the inferior frontal gyrus, and ‘lingual’ as the medial occipital region. This systematic bias toward depth in single-dipole fitting is due to the fact that ‘the large spatial extent of the many dipole layers that evidently generate EEG disqualifies them as single dipoles’(Nunez and Srinivasan, 2006). If this is the case, estimating shallower source regions along a radial direction as suggested here should provide a reasonable heuristic correction. Individual IC × IC connectivity matrix was thus mapped to a 76 × 76 custom anatomical region matrix, on which RPDC was also mapped as a weighting factor to modulate pairwise dipole density to calculate the graph edges. For both groups, including a minimum of 80% of unique subjects was set to be an inclusion criterion for each graph node to be analyzed in the next stage. Also, for group comparisons, 47/76 graph nodes showed overlap between the groups, which explained 79.3% of the total dipole density (c.f., Loo et al., 2019; Koshiyama et al., 2020d). Lastly, the 35–45 Hz was selected as the frequency range of interest, consistent with previous gamma-band ASSR studies (Koshiyama et al., 2018b, 2018c, 2019; Tada et al., 2016). For the statistics of time-frequency decomposed RPDC within- and across-groups, a weak family-wise error rate control was applied (Groppe et al., 2011; Nichols and Hayasaka, 2003).

3. Results

Both groups showed multiple ASSR source interactions that were broadly distributed across brain regions. The connectivity matrix and movies of healthy comparison subjects (Supplementary Fig. 1 and Supplementary Movie 1, 2) and schizophrenia patients (Supplementary Fig. 2 and Supplementary Movie 3, 4) are shown in the supplementary information. The connectivity matrix that represents the group-difference of gamma-band ASSR with the initial results ($p < 0.05$, corrected; two-tailed) is shown in Fig. 1. A predefined p-value threshold of $p < 0.0001$ (corrected, two-tailed (Koshiyama et al., 2020d)) revealed 15 graph edges (Fig. 2, Supplementary Fig. 3. and Supplementary Movie 5, 6).

3.1. Neural network dynamics

Neural networks consisting of increased/decreased effective connectivity underlying gamma oscillation in schizophrenia patients relative to healthy comparison subjects are shown in

Fig. 3A. This network figure shows the rank order latency of each connectivity along with Fig. 3B. Shortly after the response onset, a significant increase in connectivity was observed from the temporal to the frontal regions in schizophrenia patients (8 in Fig. 3B), followed by decreased connectivities within prefrontal regions (10, 12, 13 in Fig. 3B), described below.

3.2. Early ASSR time interval: network centered at superior temporal gyrus

Schizophrenia patients showed abnormal connectivity during the onset interval of ASSR (i.e., ~1–200 ms). Specifically, patients showed increased connectivity from the right inferior frontal gyrus to the right superior temporal gyrus (Fig. 2A and Fig. 3B). Following response onset, connectivity from the right superior temporal gyrus to the ventral middle-cingulate gyrus was decreased in patients relative to healthy comparison subjects (~100 ms to 300–400 ms). Patients also showed large increases in connectivity from the right supplementary motor area to the left inferior frontal region compared to healthy comparison subjects.

3.3. Middle time interval: connectivity from inferior frontal to occipital regions

In the 200–300 ms response interval, connectivities from the right ventral middle cingulate gyrus to the right occipital regions (i.e., the right medial occipital region and a region near the right calcarine sulcus) and from the right inferior frontal gyrus to the right medial occipital region were decreased in schizophrenia patients compared to healthy comparison subjects. These reductions persisted into the later interval of ASSR (Fig. 2B and Fig. 3B).

3.4. Later time interval: network centered at prefrontal regions

During the later phase of ASSR (i.e., 300–500 ms), patients showed significantly increased connectivity from the superior temporal gyrus to the middle frontal gyrus, followed by decreased connectivity from the left superior frontal gyrus to the right superior and middle frontal gyri. Schizophrenia related decreased connectivity included the connectivities from the right parietal (supramarginal) cortex to the left inferior frontal regions. This time interval was characterized by prominent and broad reductions in connectivity across prefrontal regions in schizophrenia patients (Fig. 2C and Fig. 3B).

4. Discussion

Results of this study characterize effective connectivities underlying gamma synchronization via a novel Granger causality analysis (Granger, 1969) applied to EEG recordings obtained from large cohorts of schizophrenia patients and healthy comparison subjects. Healthy comparison subjects and schizophrenia patients showed multiple interactions that were distributed across multiple brain regions. Gamma-band ASSR deficits in schizophrenia patients are evident at the superior temporal gyrus at the onset of the response that then cascades “forward” to yield widespread abnormalities in the engagement of prefrontal brain regions in the later intervals of the response (Fig. 4).

The present study supports the increasing use of temporally distinct ASSR time intervals in studies of patients with psychosis. In this context, early and later time intervals of gamma oscillation appear to reflect dissociable response intervals (Koshiyama et al., 2018b; Light et al., 2006, 2017; Tada et al., 2016). According to the prior studies, while first-episode

schizophrenia patients showed gamma-band ASSR deficits both in the early and later intervals, individuals with clinical high-risk for psychosis showed reductions only in the later time interval. The local neural network centered at the superior temporal gyrus in the early onset time interval may be preserved in individuals with clinical high-risk for psychosis, consistent with the progressive volume reduction within the superior temporal gyrus observed after the onset of schizophrenia in first-episode schizophrenia patients (Kasai et al., 2003a, 2003b). As hypothesized, the observed prefrontal gamma connectivity decrease during the later time interval in schizophrenia patients may reflect severe structural alterations in both gray and white matter in the frontal regions (Kelly et al., 2018; Koshiyama et al., 2018a, 2020c; van Erp et al., 2018). The present study also extended prior results by classification of the middle portion of ASSR, which represents the transition after mounting a coherent response onset to sustaining this response during the stimulation period.

Support for the use of distinct time intervals also comes from an experimental medicine trial which revealed distinct pharmacodynamic results over the later maintenance, but not early-onset phase of ASSR response in both healthy subjects and schizophrenia patients. Specifically, we reported that a single dose of the non-competitive NMDA receptor modulator, memantine, robustly increased (i.e., normalized) ASSR over later time intervals in schizophrenia patients (Light et al., 2017). Therefore, our results expanded the previous findings and provided temporal and spatial resolutions to future pre-clinical animal model studies, which will strengthen the utility of gamma-band ASSR as a translational brain marker of neuropsychiatric diseases in the development of novel therapeutic interventions.

Results of this study should be considered in the context of several limitations. First, this is a cross-sectional cohort study of a heterogeneous sample of schizophrenia patients, the majority of whom were receiving complex medication regimens. As is the case for most large-scale studies of schizophrenia patients, the medication, psychosocial environments, and other important factors that could potentially influence brain function were not experimentally controlled. Second, the schizophrenia patients in this study had a well-established illness; results, therefore, may not generalize to at-risk, early-illness psychosis, or unmedicated patients. Third, only 40 EEG channels were available for connectivity analyses in this archival cohort. While large well-characterized cohorts lend themselves to validating novel methodologic approaches, higher density recordings with at least 64 channels are recommended for future studies (Light et al., 2020; Light and Swerdlow, 2020). Moreover, individual MRI data, and digitized scalp sensor locations rather than template head models and reliance on standardized electrode locations may potentially improve the accuracy of source dynamics. Fourth, the reported effective connectivity analyses are merely descriptive and illustrative; they do not tell us about the functional roles of connectivity patterns or the functional consequences of observed abnormalities in patients. Fifth, the participants watched a silent cartoon video during ASSR measuring. While this task helped mitigate against subjects falling asleep or potential motion artifacts from subject boredom, we cannot exclude the possibility of detecting erroneous connectivities from watching the video rather than the 40-Hz auditory stimulation (e.g., occipital regions including calcarine sulcus centered at primary visual cortex). Finally, the abnormal connectivities detected in

schizophrenia patients may not be specific to schizophrenia patients; additional studies of transdiagnostic patient groups are necessary.

5. Conclusion

This study characterizes the entrainment and propagation of gamma frequency oscillations in healthy subjects and schizophrenia patients in real-time by applying a novel multivariate Granger causality analysis to large-scale scalp EEG datasets. Findings provide evidence that relatively circumscribed abnormalities in the processing of simple 40-Hz auditory stimuli at the superior temporal gyrus in schizophrenia patients rapidly cascade forward to produce widespread failures to engage distributed prefrontal brain regions that are necessary to support gamma oscillations. Deficits in the generation and maintenance of stimulus-driven gamma-band oscillations reflect a fundamental connectivity abnormality across a distributed network of the temporal and frontal regions. Clarification of the neural mechanisms underlying the networks detected in this study, in both future clinical and animal studies, will strengthen the utility of gamma-band ASSR as a translational brain marker of neuropsychiatric disorders. Additional studies are needed to validate potential applications of these EEG-based connectivity analyses as translational biomarkers in the context of novel drug and behavioral therapeutic interventions for neuropsychiatric disorders.

Supplementary Material

Refer to Web version on PubMed Central for supplementary material.

Acknowledgements

This study was supported by JSPS Overseas Research Fellowships (D. Koshiyama), Sidney R. Baer, Jr. Foundation, and NIMH grants MH042228 and MH079777. Swartz Center for Computational Neuroscience is supported by generous gift of Swartz Foundation. The funders had no role in the study design, data collection and analysis, publication decision, or manuscript preparation.

References

Akbarian S, Huang HS, 2006. Molecular and cellular mechanisms of altered GAD1/GAD67 expression in schizophrenia and related disorders. Brain Res. Rev. 52, 293–304. [PubMed: 16759710]

Andreasen NC, 1999. A unitary model of schizophrenia: Bleuler's "fragmented phrene" as schizencephaly. Arch. Gen. Psychiatry 56, 781–787. [PubMed: 12884883]

Blum S, Jacobsen NSJ, Bleichner MG, Debener S, 2019. A Riemannian modification of Artifact subspace reconstruction for EEG Artifact handling. Front. Hum. Neurosci. 13, 141. [PubMed: 31105543]

Braff DL, 1993. Information processing and attention dysfunctions in schizophrenia. Schizophr. Bull. 19, 233–259. [PubMed: 8322034]

Braff D, Stone C, Callaway E, Geyer M, Glick I, Bali L, 1978. Prestimulus effects on human startle reflex in normals and schizophrenics. Psychophysiology 15, 339–343. [PubMed: 693742]

Brenner CA, Sporns O, Lysaker PH, O'Donnell BF, 2003. EEG synchronization to modulated auditory tones in schizophrenia, schizoaffective disorder, and schizotypal personality disorder. Am. J. Psychiatry 160, 2238–2240. [PubMed: 14638599]

Cardin JA, Carlen M, Meletis K, Knoblich U, Zhang F, Deisseroth K, et al. , 2009. Driving fast-spiking cells induces gamma rhythm and controls sensory responses. Nature 459, 663–667. [PubMed: 19396156]

Carlen M, Meletis K, Siegle JH, Cardin JA, Futai K, Vierling-Claassen D, et al. , 2012. A critical role for NMDA receptors in parvalbumin interneurons for gamma rhythm induction and behavior. Mol. Psychiatry 17, 537–548. [PubMed: 21468034]

Chan RC, Di X, McAlonan GM, Gong QY, 2011. Brain anatomical abnormalities in high-risk individuals, first-episode, and chronic schizophrenia: an activation likelihood estimation meta-analysis of illness progression. Schizophr. Bull. 37, 177–188. [PubMed: 19633214]

Chang CY, Hsu SH, Pion-Tonachini L, Jung TP, 2018. Evaluation of artifact subspace reconstruction for automatic EEG Artifact removal. Conf. Proc. IEEE Eng. Med. Biol. Soc. 2018, 1242–1245.

Chang CY, Hsu SH, Pion-Tonachini L, Jung TP, 2020. Evaluation of artifact subspace reconstruction for automatic artifact components removal in multi-channel EEG recordings. IEEE Trans. Biomed. Eng. 67, 1114–1121. [PubMed: 31329105]

Delorme A, Makeig S, 2004. EEGLAB: an open source toolbox for analysis of single-trial EEG dynamics including independent component analysis. J. Neurosci. Methods 134, 9–21. [PubMed: 15102499]

Delorme A, Palmer J, Onton J, Oostenveld R, Makeig S, 2012. Independent EEG sources are dipolar. PLoS One 7, e30135. [PubMed: 22355308]

Desai A, Benner L, Wu R, Gertsik L, Maruff P, Light GA, et al. , 2020. Phase 1 randomized study on the safety, tolerability, and pharmacodynamic cognitive and electrophysiological effects of a dopamine D_1 receptor positive allosteric modulator in patients with schizophrenia. Neuropsychopharmacology in press.

Edgar JC, Chen YH, Lanza M, Howell B, Chow VY, Heiken K, et al. , 2014. Cortical thickness as a contributor to abnormal oscillations in schizophrenia? Neuroimage Clin. 4, 122–129. [PubMed: 24371794]

Edgar JC, Fisk Clt, Liu S, Pandey J, Herrington JD, Schultz RT, et al. , 2016. Translating adult electrophysiology findings to younger patient populations: difficulty measuring 40-Hz auditory steady-state responses in typically developing children and children with autism spectrum disorder. Dev. Neurosci. 38, 1–14. [PubMed: 26730806]

Eyles DW, McGrath JJ, Reynolds GP, 2002. Neuronal calcium-binding proteins and schizophrenia. Schizophr. Res. 57, 27–34. [PubMed: 12165373]

Fisahn A, Neddens J, Yan L, Buonanno A, 2009. Neuregulin-1 modulates hippocampal gamma oscillations: implications for schizophrenia. Cereb. Cortex 19, 612–618. [PubMed: 18632742]

Gabard-Durnam LJ, Mendez Leal AS, Wilkinson CL, Levin AR, 2018. The Harvard automated processing pipeline for electroencephalography (HAPPE): standardized processing software for developmental and high-artifact data. Front. Neurosci. 12, 97. [PubMed: 29535597]

Galambos R, Makeig S, 1992. Physiological studies of central masking in man. I: the effects of noise on the 40-Hz steady-state response. J. Acoust. Soc. Am. 92, 2683–2690. [PubMed: 1479130]

Galambos R, Makeig S, Talmachoff PJ, 1981. A 40-Hz auditory potential recorded from the human scalp. Proc. Natl. Acad. Sci. U. S. A. 78, 2643–2647. [PubMed: 6941317]

Galuske RAW, Munk MHJ, Singer W, 2019. Relation between gamma oscillations and neuronal plasticity in the visual cortex. Proc. Natl. Acad. Sci. U. S. A. 116, 23317–23325. [PubMed: 31659040]

Gandal MJ, Edgar JC, Klook K, Siegel SJ, 2012. Gamma synchrony: towards a translational biomarker for the treatment-resistant symptoms of schizophrenia. Neuropharmacology 62, 1504–1518. [PubMed: 21349276]

Gonzalez-Burgos G, Cho RY, Lewis DA, 2015. Alterations in cortical network oscillations and parvalbumin neurons in schizophrenia. Biol. Psychiatry 77, 1031–1040. [PubMed: 25863358]

Granger CWJ, 1969. Investigating causal relations by econometric models and cross-spectral methods. Econometrica 37, 424–438.

Groppe DM, Urbach TP, Kutas M, 2011. Mass univariate analysis of event-related brain potentials/fields I: a critical tutorial review. Psychophysiology 48, 1711–1725. [PubMed: 21895683]

Hagoort P, Hald L, Bastiaansen M, Petersson KM, 2004. Integration of word meaning and world knowledge in language comprehension. Science 304, 438–441. [PubMed: 15031438]

Hamm JP, Bobilev AM, Hayrynen LK, Hudgens-Haney ME, Oliver WT, Parker DA, et al. , 2015. Stimulus train duration but not attention moderates gamma-band entrainment abnormalities in schizophrenia. Schizophr. Res. 165, 97–102. [PubMed: 25868936]

Hirano Y, Oribe N, Kanba S, Onitsuka T, Nestor PG, Spencer KM, 2015. Spontaneous gamma activity in schizophrenia. JAMA Psychiatry 72, 813–821. [PubMed: 25587799]

Isomura S, Onitsuka T, Tsuchimoto R, Nakamura I, Hirano S, Oda Y, et al. , 2016. Differentiation between major depressive disorder and bipolar disorder by auditory steady-state responses. J. Affect. Disord. 190, 800–806. [PubMed: 26625092]

Joliot M, Ribary U, Llinas R, 1994. Human oscillatory brain activity near 40 Hz coexists with cognitive temporal binding. Proc. Natl. Acad. Sci. U. S. A. 91, 11748–11751. [PubMed: 7972135]

Kasai K, Shenton ME, Salisbury DF, Hirayasu Y, Lee CU, Ciszewski AA, et al. , 2003a. Progressive decrease of left superior temporal gyrus gray matter volume in patients with first-episode schizophrenia. Am. J. Psychiatry 160, 156–164. [PubMed: 12505815]

Kasai K, Shenton ME, Salisbury DF, Hirayasu Y, Onitsuka T, Spencer MH, et al. , 2003b. Progressive decrease of left Heschl gyrus and planum temporale gray matter volume in first-episode schizophrenia: a longitudinal magnetic resonance imaging study. Arch. Gen. Psychiatry 60, 766–775. [PubMed: 12912760]

Kelly S, Jahanshad N, Zalesky A, Kochunov P, Agartz I, Alloza C, et al., 2018. Widespread White Matter Microstructural Differences in Schizophrenia across 4322 Individuals: Results from the ENIGMA Schizophrenia DTI Working Group, 23, pp. 1261–1269.

Koshiyama D, Fukunaga M, Okada N, Morita K, Nemoto K, Yamashita F, et al. , 2018a. Role of frontal white matter and corpus callosum on social function in schizophrenia. Schizophr. Res. 202, 180–187. [PubMed: 30005932]

Koshiyama D, Kirihara K, Tada M, Nagai T, Fujioka M, Ichikawa E, et al. , 2018b. Auditory gamma oscillations predict global symptomatic outcome in the early stages of psychosis: a longitudinal investigation. Clin. Neurophysiol. 129, 2268–2275. [PubMed: 30216911]

Koshiyama D, Kirihara K, Tada M, Nagai T, Fujioka M, Ichikawa E, et al. , 2018c. Electrophysiological evidence for abnormal glutamate-GABA association following psychosis onset. Transl. Psychiatry 8, 211. [PubMed: 30297786]

Koshiyama D, Kirihara K, Tada M, Nagai T, Fujioka M, Usui K, et al. , 2019. Gamma-band auditory steady-state response is associated with plasma levels of d-serine in schizophrenia: an exploratory study. Schizophr. Res. 208, 467–469. [PubMed: 30819595]

Koshiyama D, Miyakoshi M, Thomas ML, Joshi YB, Molina JL, Tanaka-Koshiyama K, et al. , 2020a. Auditory-based cognitive training drives short- and long-term plasticity in cortical networks in schizophrenia. Schizophr. Bull. Open. 10.1093/schizbullopen/sgaa065 (in press).

Koshiyama D, Thomas ML, Miyakoshi M, Joshi YB, Molina JL, Tanaka-Koshiyama K, et al. , 2020b. Hierarchical pathways from sensory processing to cognitive, clinical, and functional impairments in schizophrenia. Schizophr. Bull. 10.1093/schbul/sbaa116 in press.

Koshiyama D, Fukunaga M, Okada N, Morita K, Nemoto K, Usui K, et al. , 2020c. White matter microstructural alterations across four major psychiatric disorders: mega-analysis study in 2937 individuals. Mol. Psychiatry 25, 883–895. [PubMed: 31780770]

Koshiyama D, Miyakoshi M, Joshi YB, Molina JL, Tanaka-Koshiyama K, Sprock J, et al. , 2020d. Abnormal effective connectivity underlying auditory mismatch negativity impairments in schizophrenia. Biol. Psychiary Cogn. Neurosci. Neuroimaging. 5, 1028–1039.

Koshiyama D, Miyakoshi M, Joshi YB, Molina JL, Tanaka-Koshiyama K, Sprock J, et al. , 2020e. A distributed frontotemporal network underlies gamma-band synchronization impairments in schizophrenia patients. Neuropsychopharmacology 45, 2198–2206. [PubMed: 32829382]

Koshiyama D, Miyakoshi M, Thomas ML, Joshi YB, Molina JL, Tanaka-Koshiyama K, et al. , 2020f. Unique contributions of sensory discrimination and gamma synchronization deficits to cognitive, clinical, and psychosocial functional impairments in schizophrenia. BioRxiv. 10.1101/2020.07.19.211193.

Kothe CA, Makeig S, 2013. BCILAB: a platform for brain-computer interface development. J. Neural Eng. 10, 056014. [PubMed: 23985960]

Kozono N, Honda S, Tada M, Kirihara K, Zhao Z, Jinde S, et al. , 2019. Auditory steady state response; nature and utility as a translational science tool. Sci. Rep. 9, 8454. [PubMed: 31186500]

Kwon JS, O'Donnell BF, Wallenstein GV, Greene RW, Hirayasu Y, Nestor PG, et al. , 1999. Gamma frequency-range abnormalities to auditory stimulation in schizophrenia. Arch. Gen. Psychiatry 56, 1001–1005. [PubMed: 10565499]

Larsen KM, Pellegrino G, Birknow MR, Kjaer TN, Baare WFC, Didriksen M, et al. , 2018. 22q11.2 Deletion syndrome is associated with impaired auditory steady-state gamma response. Schizophr. Bull. 44, 388–397. [PubMed: 28521049]

Light GA, Braff DL, 2005. Mismatch negativity deficits are associated with poor functioning in schizophrenia patients. Arch. Gen. Psychiatry 62, 127–136. [PubMed: 15699289]

Light GA, Swerdlow NR, 2020. Selection criteria for neurophysiologic biomarkers to accelerate the pace of CNS therapeutic development. Neuropsychopharmacology 45, 237–238. [PubMed: 31506611]

Light GA, Hsu JL, Hsieh MH, Meyer-Gomes K, Sprock J, Swerdlow NR, et al. , 2006. Gamma band oscillations reveal neural network cortical coherence dysfunction in schizophrenia patients. Biol. Psychiatry 60, 1231–1240. [PubMed: 16893524]

Light GA, Zhang W, Joshi YB, Bhakta S, 2017. Single-dose memantine improves cortical oscillatory response dynamics in patients with schizophrenia. Neuropsychopharmacology 42, 2633–2639. [PubMed: 28425497]

Light GA, Joshi YB, Molina J, Bhakta SG, Nungaray JA, Cardoso L, et al. , 2020. Neurophysiological biomarkers for schizophrenia therapeutics. Biomark. Neuropsychiatry 2, 100012.

Loo SK, Miyakoshi M, Tung K, Lloyd E, Salgari G, Dillon A, et al. , 2019. Neural activation and connectivity during cued eye blinks in chronic tic disorders. Neuroimage Clin. 24, 101956. [PubMed: 31382238]

Makeig S, 1993. Auditory event-related dynamics of the EEG spectrum and effects of exposure to tones. Electroencephalogr. Clin. Neurophysiol. 86, 283–293. [PubMed: 7682932]

Miltner WH, Braun C, Arnold M, Witte H, Taub E, 1999. Coherence of gamma-band EEG activity as a basis for associative learning. Nature 397, 434–436. [PubMed: 9989409]

Molina JL, Thomas ML, Joshi YB, Hochberger WC, Koshiyama D, Nungaray JA, et al. , 2020. Gamma oscillations predict pro-cognitive and clinical response to auditory-based cognitive training in schizophrenia. Transl. Psychiatry 10, 405. [PubMed: 33230190]

Mullen TR, Kothe CA, Chi YM, Ojeda A, Kerth T, Makeig S, et al. , 2015. Real-time neuroimaging and cognitive monitoring using wearable dry EEG. IEEE Trans. Biomed. Eng. 62, 2553–2567. [PubMed: 26415149]

Nakao K, Nakazawa K, 2014. Brain state-dependent abnormal LFP activity in the auditory cortex of a schizophrenia mouse model. Front. Neurosci. 8, 168. [PubMed: 25018691]

Nichols T, Hayasaka S, 2003. Controlling the familywise error rate in functional neuroimaging: a comparative review. Stat. Methods Med. Res. 12, 419–446. [PubMed: 14599004]

Nunez P, Srinivasan R, 2006. Electric Fields of the Brain. Oxford University Press, New York.

Oda Y, Onitsuka T, Tsuchimoto R, Hirano S, Oribe N, Ueno T, et al. , 2012. Gamma band neural synchronization deficits for auditory steady state responses in bipolar disorder patients. PLoS One 7, e39955. [PubMed: 22792199]

O'Donnell BF, Hetrick WP, Vohs JL, Krishnan GP, Carroll CA, Shekhar A, 2004. Neural synchronization deficits to auditory stimulation in bipolar disorder. Neuroreport 15, 1369–1372. [PubMed: 15167568]

Oostenveld R, Praamstra P, 2001. The five percent electrode system for high-resolution EEG and ERP measurements. Clin. Neurophysiol. 112, 713–719. [PubMed: 11275545]

Oostenveld R, Fries P, Maris E, Schoffelen JM, 2011. FieldTrip: open source software for advanced analysis of MEG, EEG, and invasive electrophysiological data. Comput. Intell. Neurosci. 2011, 156869. [PubMed: 21253357]

Piazza C, Miyakoshi M, Akalin-Acar Z, Cantiani C, Reni G, Bianchi AM, 2016. An Automated Function for Identifying EEG Independent Components Representing Bilateral Source Activity.

XIV Mediterranean Conference on Medical and Biological Engineering and Computing 2016. Springer International Publishing, pp. 105–109.

Pion-Tonachini L, Kreutz-Delgado K, Makeig S, 2019. ICLabel: an automated electroencephalographic independent component classifier, dataset, and website. Neuroimage 198, 181–197. [PubMed: 31103785]

Rass O, Krishnan G, Brenner CA, Hetrick WP, Merrill CC, Shekhar A, et al. , 2010. Auditory steady state response in bipolar disorder: relation to clinical state, cognitive performance, medication status, and substance disorders. Bipolar Disord. 12, 793–803. [PubMed: 21176026]

Reite M, Teale P, Rojas DC, Reite E, Asherin R, Hernandez O, 2009. MEG auditory evoked fields suggest altered structural/functional asymmetry in primary but not secondary auditory cortex in bipolar disorder. Bipolar Disord. 11, 371–381. [PubMed: 19500090]

Rodriguez E, George N, Lachaux JP, Martinerie J, Renault B, Varela FJ, 1999. Perception's shadow: long-distance synchronization of human brain activity. Nature 397, 430–433. [PubMed: 9989408]

Schelter B, Timmer J, Eichler M, 2009. Assessing the strength of directed influences among neural signals using renormalized partial directed coherence. J. Neurosci. Methods 179, 121–130. [PubMed: 19428518]

Sohal VS, Zhang F, Yizhar O, Deisseroth K, 2009. Parvalbumin neurons and gamma rhythms enhance cortical circuit performance. Nature 459, 698–702. [PubMed: 19396159]

Spellman T, Rigotti M, Ahmari SE, Fusi S, Gogos JA, Gordon JA, 2015. Hippocampal-prefrontal input supports spatial encoding in working memory. Nature 522, 309–314. [PubMed: 26053122]

Spencer KM, Nestor PG, Perlmutter R, Niznikiewicz MA, Klump MC, Frumin M, et al. , 2004. Neural synchrony indexes disordered perception and cognition in schizophrenia. Proc. Natl. Acad. Sci. U. S. A. 101, 17288–17293. [PubMed: 15546988]

Spencer KM, Salisbury DF, Shenton ME, McCarley RW, 2008. Gamma-band auditory steady-state responses are impaired in first episode psychosis. Biol. Psychiatry 64, 369–375. [PubMed: 18400208]

Sun Y, Farzan F, Barr MS, Kirihara K, Fitzgerald PB, Light GA, et al. , 2011. Gamma oscillations in schizophrenia: mechanisms and clinical significance. Brain Res. 1413, 98–114. [PubMed: 21840506]

Tada M, Nagai T, Kirihara K, Koike S, Suga M, Araki T, et al. , 2016. Differential alterations of auditory gamma oscillatory responses between pre-onset high-risk individuals and first-episode schizophrenia. Cereb. Cortex 26, 1027–1035. [PubMed: 25452567]

Teale P, Collins D, Maharajh K, Rojas DC, Kronberg E, Reite M, 2008. Cortical source estimates of gamma band amplitude and phase are different in schizophrenia. Neuroimage 42, 1481–1489. [PubMed: 18634887]

Thune H, Recasens M, Uhlhaas PJ, 2016. The 40-Hz auditory steady-state response in patients with schizophrenia: a meta-analysis. JAMA Psychiatry 73, 1145–1153. [PubMed: 27732692]

Traub RD, Whittington MA, Stanford IM, Jefferys JG, 1996. A mechanism for generation of long-range synchronous fast oscillations in the cortex. Nature 383, 621–624. [PubMed: 8857537]

Tsuchimoto R, Kanba S, Hirano S, Oribe N, Ueno T, Hirano Y, et al. , 2011. Reduced high and low frequency gamma synchronization in patients with chronic schizophrenia. Schizophr. Res. 133, 99–105. [PubMed: 21849245]

Tzourio-Mazoyer N, Landeau B, Papathanassiou D, Crivello F, Etard O, Delcroix N, et al. , 2002. Automated anatomical labeling of activations in SPM using a macroscopic anatomical parcellation of the MNI MRI single-subject brain. Neuroimage 15, 273–289. [PubMed: 11771995]

Uhlhaas PJ, Singer W, 2010. Abnormal neural oscillations and synchrony in schizophrenia. Nat. Rev. Neurosci. 11, 100–113. [PubMed: 20087360]

Uhlhaas PJ, Singer W, 2015. Oscillations and neuronal dynamics in schizophrenia: the search for basic symptoms and translational opportunities. Biol. Psychiatry 77, 1001–1009. [PubMed: 25676489]

Uhlhaas PJ, Haenschel C, Nikolic D, Singer W, 2008. The role of oscillations and synchrony in cortical networks and their putative relevance for the pathophysiology of schizophrenia. Schizophr. Bull. 34, 927–943. [PubMed: 18562344]

van Erp TGM, Walton E, Hibar DP, Schmaal L, Jiang W, Glahn DC, et al. , 2018. Cortical brain abnormalities in 4474 individuals with schizophrenia and 5098 control subjects via the enhancing

neuro imaging genetics through Meta analysis (ENIGMA) consortium. Biol. Psychiatry 84, 644–654. [PubMed: 29960671]

Vierling-Claassen D, Siekmeier P, Stufflebeam S, Kopell N, 2008. Modeling GABA alterations in schizophrenia: a link between impaired inhibition and altered gamma and beta range auditory entrainment. J. Neurophysiol. 99, 2656–2671. [PubMed: 18287555]

Wilson TW, Hernandez OO, Asherin RM, Teale PD, Reite ML, Rojas DC, 2008. Cortical gamma generators suggest abnormal auditory circuitry in early-onset psychosis. Cereb. Cortex 18, 371–378. [PubMed: 17557901]

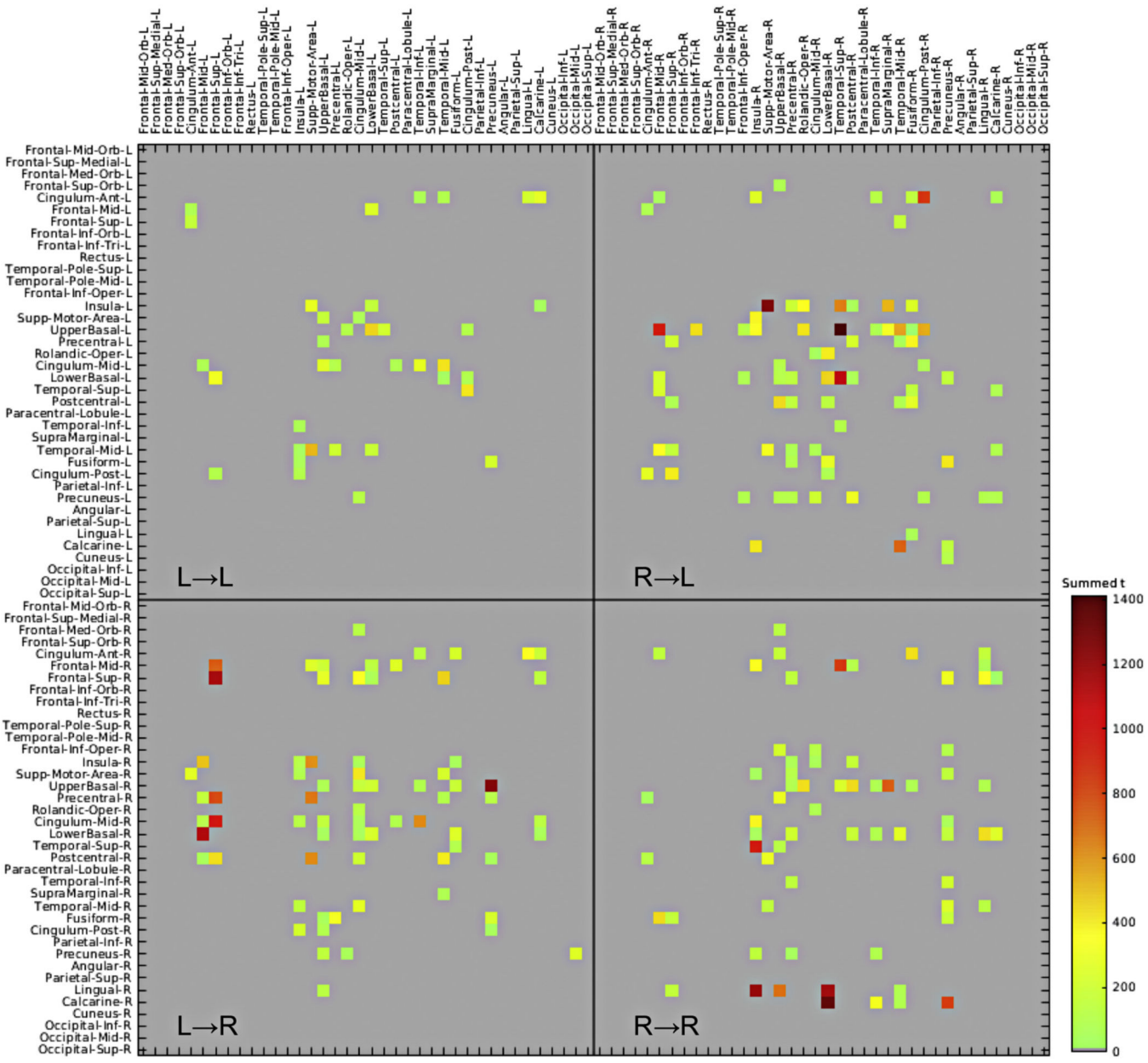

Fig. 1.

Connectivity matrix of 76 × 76 anatomical region of interests (ROIs) that represents the group-difference.

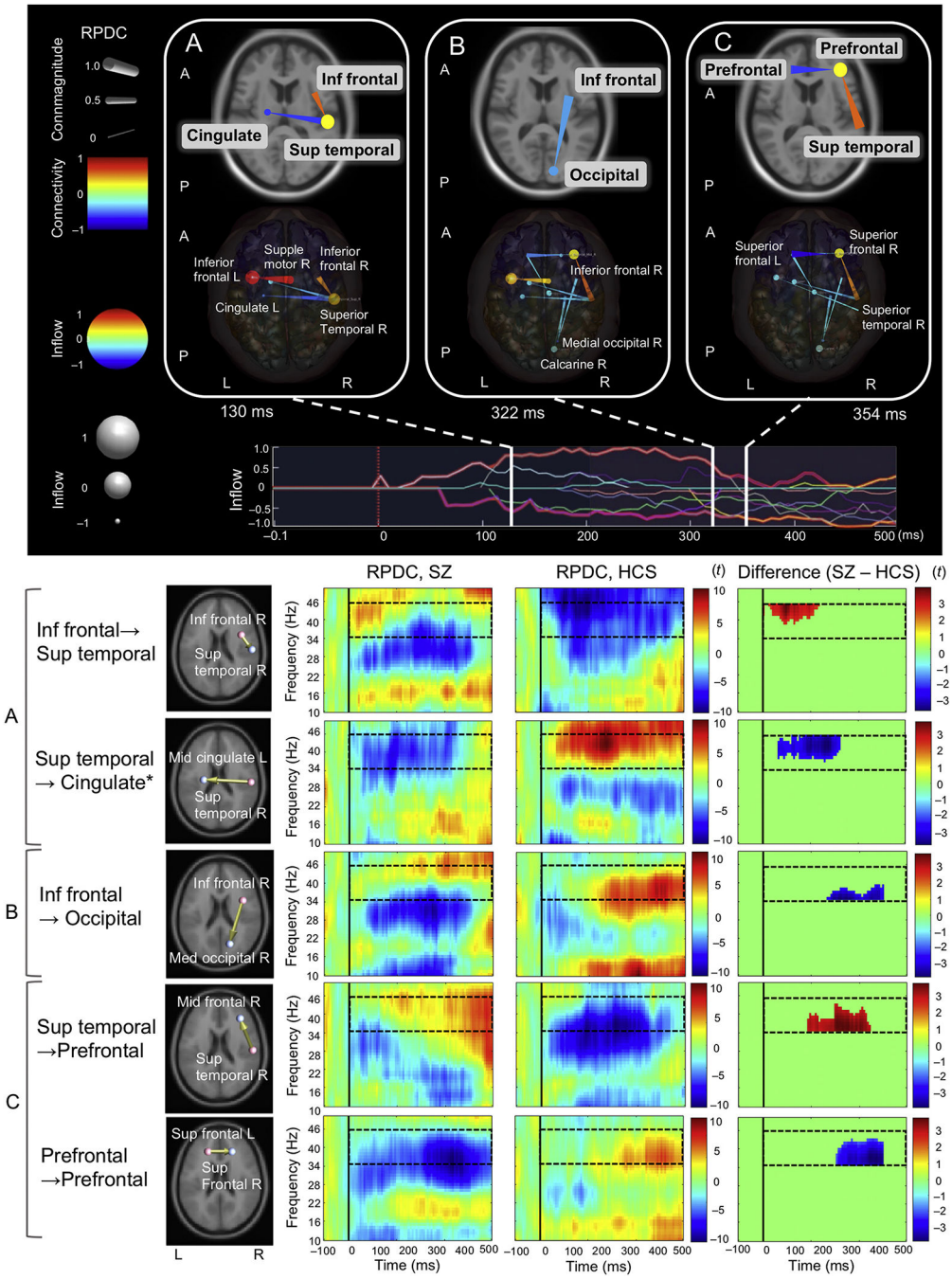

Fig. 2. Difference of effective connectivity between schizophrenia and healthy comparison subject groups.

Note: Lower row of brain images indicates one frame of the effective connectivity movie at 130 ms (A), 322 ms (B) 354 ms (C) after the stimulus onset seen from an axial view (Supplementary Movie 1 and 2); upper row of brain images indicates main findings of connectivity; the panel shows the envelope of the significant edges between 35 and 45 Hz; lower part of the figure shows the five major areas of connectivity; solid black line at Latency = 0 is the stimulus onset; broken black line indicates region of interest between 35

and 45 Hz and between 0 and 500 ms; * the original label is ‘lower basal’ (refer to Methods section).

Abbreviations: RPDC, renormalized partial directed coherence; Inf frontal; inferior frontal; Sup temporal; superior temporal; Supple motor; supplementary motor area; SZ, schizophrenia; HCS, healthy comparison subject; A, anterior; P, posterior; L, left; R, right.

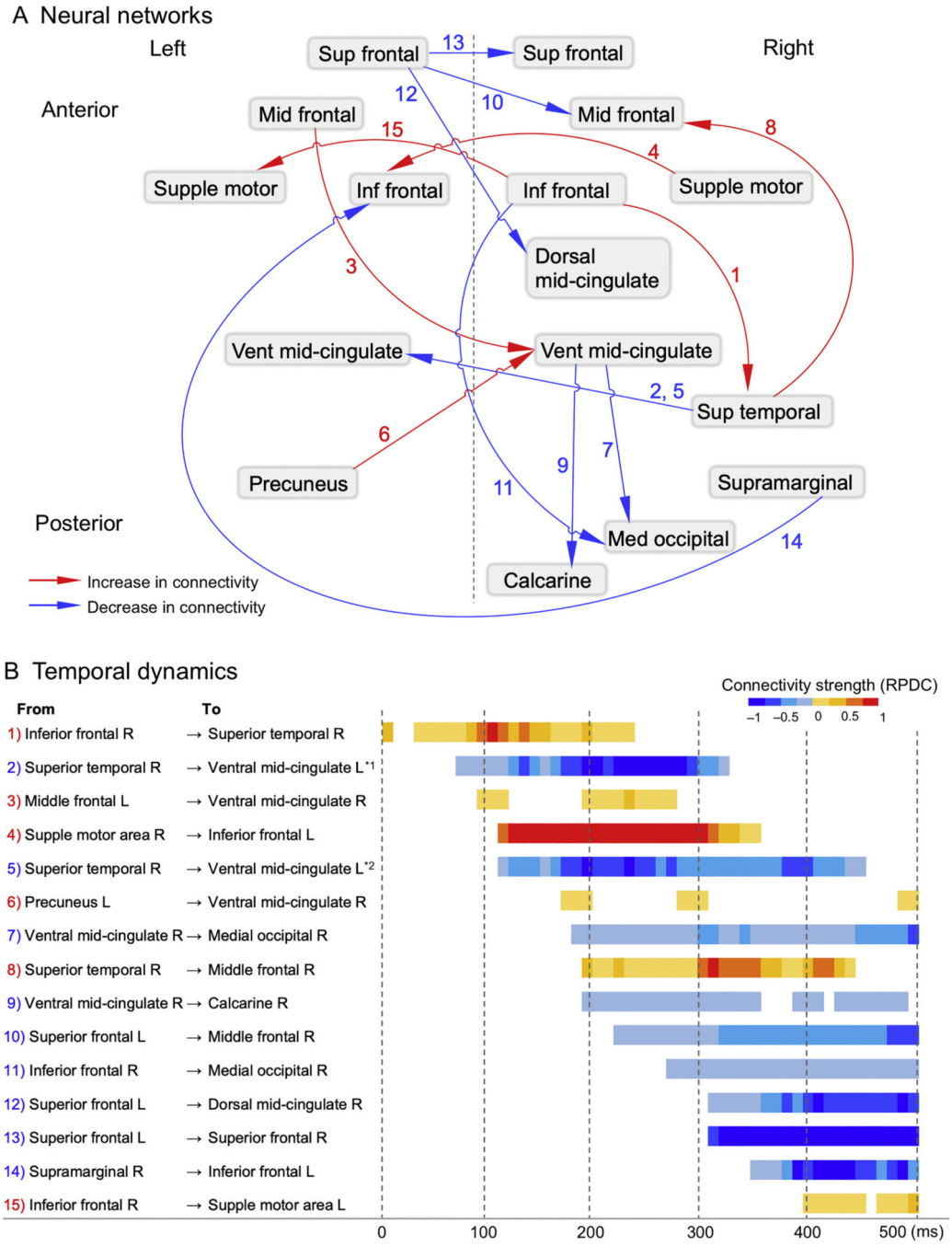

Fig. 3. Neural networks (A) and temporal dynamics (B) consisting of increased/decreased effective connectivity underlying gamma oscillation in schizophrenia patients relative to healthy comparison subjects.

Note: The numbers indicate rank order latency of each connectivity; *1 the original label is 'lower basal'; *2 the original label is 'upper basal' (refer to Methods section). Abbreviations: Sup frontal; superior frontal; Mid frontal; middle frontal; Supple motor, supplementary motor area; Inf frontal, inferior frontal; Dorsal mid-cingulate; dorsal middle cingulate; Vent mid-cingulate, ventral middle cingulate; Sup temporal; superior temporal; Med occipital, medial occipital; RPDC, renormalized partial directed coherence; L, left; R, right.

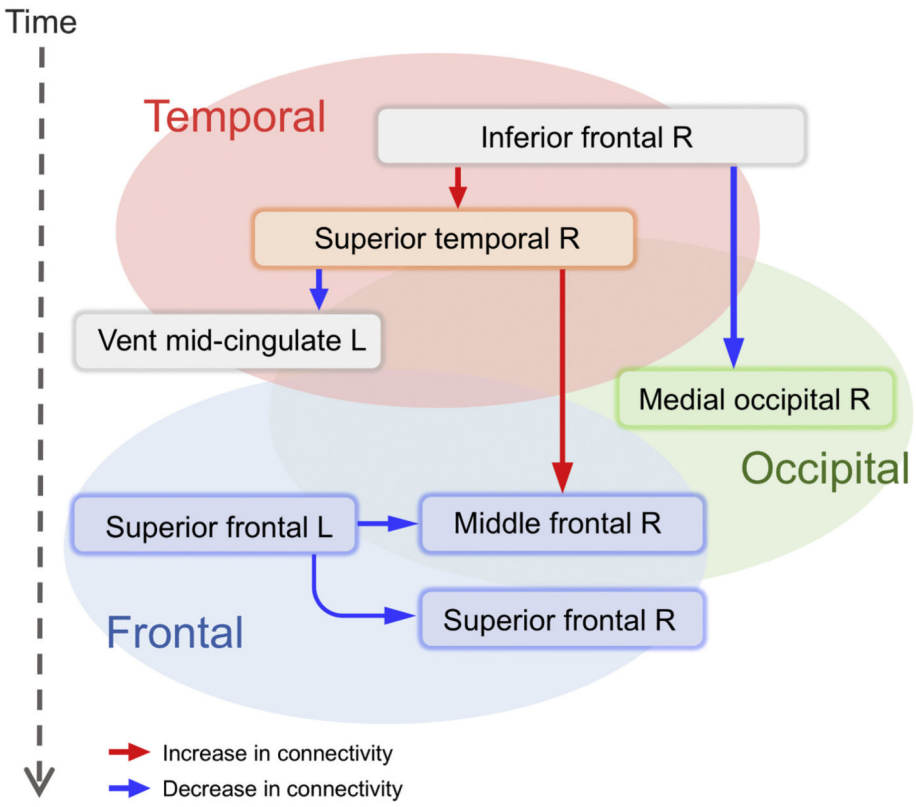

Fig. 4.

Abnormal neural networks in schizophrenia patients at the superior temporal gyrus in early portion of the response and at the prefrontal gyrus in later portion.

Table 1

Demographic and clinical characteristics of subjects.

	Healthy comparison subjects (*n* = 293)		Schizophrenia patients (*n* = 426)	
	Mean	**SD**	**Mean**	**SD**
Gender (male/female)	141/152	–	309/117	–
Age (years)	44.7	11.4	45.5	9.5
Education (years)	14.9	2.3	12.0	2.2
Duration of illness (years) [a]	–	–	23.7	10.1
SAPS total score[b]	–	–	8.9	4.1
SANS total score[b]	–	–	14.3	4.3
GAF[c]	–	–	40.9	6.6

Note:

[a]Three subjects have no data of duration of illness

[b]Four subjects have no SAPS or SANS data

[c]One subject has no GAF data.

Abbreviations: SAPS, Scale for the Assessment of Positive Symptoms; SANS, Scale for the Assessment of Negative Symptoms.